Environmental Biology of Fishes **67:** 321–339, 2003.

Electric signal variation among seven blunt-snouted *Brienomyrus* species (Teleostei: Mormyridae) from a riverine species flock in Gabon, Central Africa

Matthew E. Arnegard & Carl D. Hopkins
Department of Neurobiology and Behavior, Seeley G. Mudd Hall, Cornell University, Ithaca, NY 14853-2702, U.S.A. (e-mail: mea21@cornell.edu)

Received 5 September 2002 Accepted 12 April 2003

Key words: electric organ discharge, waveform landmarks, multivariate analysis, mormyrid taxonomy, species recognition

Synopsis

A recently discovered species flock of mormyrid fishes is marked by a striking degree of electric signal diversity among species of rather similar form. We investigated electric organ discharge (EOD) variation in a group of seven, morphologically similar *Brienomyrus* species within this species flock. All of these forms have blunt snouts. We made quantitative measurements of 25 EOD characters from field recorded signals. Results of principal components analyses using these characters demonstrate that distinct, species-typical EODs are produced by each of the morphologically defined blunt-snouted taxa, consistent with the hypothesis that the EOD plays a role in species recognition. We correctly assigned 30 novel individuals to species on the basis of EOD characters alone using classification functions derived from discriminant function analysis. Landmark-based ordination is a powerful technique for quantifying EOD variation and delimiting species boundaries. This approach will provide an important aid in taxonomic descriptions of new *Brienomyrus* forms that are still being discovered from the rivers and streams of Gabon.

Introduction

Numerous mate attraction signals playing a role in species recognition have been described for the acoustic/vibrational (Otte 1994, Den Hollander 1995), visual (Hunsaker 1962, Bernard & Remington 1991), and chemical (Morse & Meighen 1986, Linn & Roelofs 1995) sensory modalities. Not surprisingly, these kinds of signals can be useful taxonomic characters for distinguishing closely related animals of similar form. Male breeding coloration, for example, plays a role in species recognition in the African cichlid species flocks (Seehausen & van Alphen 1998, Couldridge & Alexander 2002). Live coloration is commonly used to diagnose closely related cichlid species, while preserved specimens may be extremely difficult to distinguish (Greenwood 1974). Similarly, scrutiny of courtship songs has uncovered morphologically cryptic taxonomic diversity in green lacewings (Henry et al. 1993) and Hawaiian crickets (Otte 1994, Shaw 2000).

African mormyrid fishes emit weak, pulse-type electric organ discharges (EODs) for the purpose of object localization and social communication (Bullock & Heiligenberg 1986, Moller 1995). EOD variation depends on the morphology and physiology of the electrocytes that constitute the mormyrid electric organ. Each of these electrocytes possesses a complex, electrically excitable stalk system that conveys spikes from electromotor synapses to the electrocyte face from which the stalks arise (Bennett 1971, Bass 1986a,b, see Figure 1b and c). By conducting playback experiments in the field, Hopkins & Bass (1981) demonstrated that temporal characteristics of the EOD mediate conspecific recognition during courtship in an undescribed *Brienomyrus* species from Gabon. A neural pathway for EOD temporal coding was subsequently described in *Brienomyrus brachyistius* (Xu-Friedman & Hopkins 1999).

Most previous studies of EOD variation in mormyrids have focused on seasonal sex differences

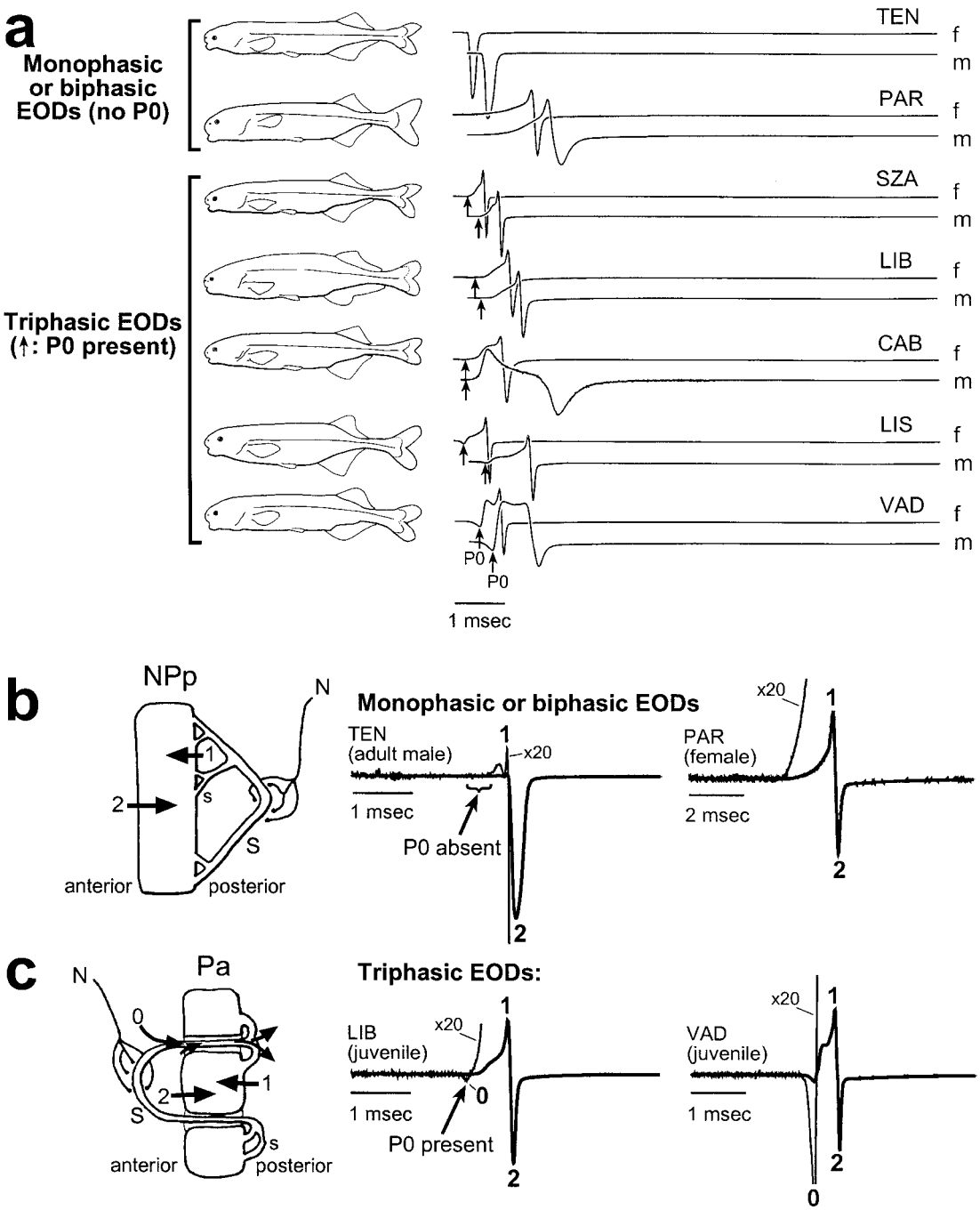

Figure 1. Seven undescribed, blunt-snouted *Brienomyrus* species from Gabon, showing their EODs and the two electrocyte types present among these species. (a) Line drawing of each species shown next to representative female and male EOD traces (all plotted on the same time base with head-positivity up). The times of occurrence of initial head-negative peaks (P0s) are indicated with arrows for the five triphasic species. Two different electrocyte types (drawn schematically) are present among these species. (b) Electrocytes with non-penetrating stalks that are innervated on the posterior side of the electrocyte (type NPp) produce mono/biphasic EODs. (c) Electrocytes with penetrating stalks that are innervated on the anterior side (type Pa) produce triphasic EODs. Net current flow through the stalk and current flow across the electrocyte faces (numbered arrows in b and c) are responsible for the different phases of the representative waveforms (shown to the right and correspondingly numbered). Radial current flow in the stalk becomes directional where the stalk penetrates the electrocyte. Amplified traces (×20) are shown to illustrate the presence or absence of small peaks in the illustrated waveforms. Electrocyte stalks and stalklets are indicated with S and s, respectively, and electromotor axons are indicated by N.

in males (Hopkins 1980, Westby & Kirschbaum 1982, Kramer 1997) or differences that are induced by treatment with androgen hormones (Bass & Hopkins 1983, 1985, Landsman et al. 1990, Herfeld & Moller 1998). Past analyses of interspecific or morphotypic EOD variation have been limited to qualitative or univariate comparisons (Gosse & Szabo 1960, Hopkins 1980, Crawford & Hopkins 1989, Moller & Brown 1990, Kramer & van der Bank 2000). These approaches have sufficed for distinguishing EODs due to the tractable number of signals under consideration or the gross differences in EOD waveform among taxa.

Here, we take a multivariate statistical approach to investigate EOD variation among seven undescribed *Brienomyrus* species with blunt snouts (Teugels & Hopkins unpublished, Figure 1a) from a recently discovered species flock that has radiated in the Ogooué River system (Hopkins 1999, Sullivan et al. 2000, 2002). Two different electrocyte types are present among these species (Figure 1b and c). Type NPp electrocytes have non-penetrating stalks that are innervated on the posterior side of each electrocyte, resulting in the production of a biphasic (or nearly monophasic) EOD in which the initial phase of EOD is always head-positive. Type Pa electrocytes have penetrating stalks that are innervated on the anterior side, resulting in the production of a triphasic EOD with a head-negative initial phase (Alves-Gomes & Hopkins 1997, Sullivan et al. 2000, 2002, Lavoué et al. 2000). We develop a quantitative method for comparing EODs among these closely related species using 25 landmark, phase area, and spectral characters. Ordinations of individuals were performed using this character set in order to: (1) rigorously test whether EOD waveform variation conforms to species boundaries which have been delineated on morphological grounds; (2) determine the accuracy with which individuals can be classified on the basis of EOD characters alone; and (3) compare EOD characters in terms of their power to discriminate among species.

Methods

Specimen collection and EOD recording

We collected a total of 280 blunt-snouted *Brienomyrus* individuals (listed in Appendix 1) between 1981 and 1999 from forested streams and rivers in different regions of Gabon (Figure 2). These specimens comprise seven undescribed mormyrid species (Figure 1a). Six of these species have previously been referred to as *Brienomyrus* species 1–5 and *Brienomyrus* species 7 (Alves-Gomes & Hopkins 1997, Hopkins 1999, Sullivan et al. 2000), but additional forms have more recently been discovered from localities throughout the Ogooué River basin, as summarized in Sullivan et al. (2002). Here, we utilized the nomenclature of Sullivan et al. (2002), which employs a three-letter code corresponding to working manuscript names proposed for these taxa (Teugels & Hopkins unpublished). All seven of these species can be distinguished morphologically from one another and from all previously described *Brienomyrus* species and are, thus, currently in the process of being formally described (Teugels & Hopkins unpublished).

Electric organ discharges were recorded from these fishes within a few hours of capture in 5–20 l plastic aquariums filled with water from the collection locality (conductivity = 12–30 μS/cm; temperature = 22–26°C). Signals were recorded with a bipolar silver/silver-chloride electrode and amplified with a BMA-831/XR differential bioamplifier (CWE, Inc.). Recordings were either DC (bandwidth = 0–50 kHz), in which case any DC offset in the electrodes and recording system was balanced out, or AC-coupled (bandwidth = 0.1–50 kHz).

Electric organ discharges were digitized using one of a number of systems: (1) a Tekronix 222 digital oscilloscope (8 bit accuracy, 512 points per recording, 1 MHz sampling rate); (2) a custom-built pulse logger (8 bit, 4096 points, 1 MHz); or (3) an IOTECH Daqbook 200 (16 bit, variable number of points, 100 kHz). Prior to 1993, analog recordings were made of EODs using a Nagra IV SJ tape recorder. These recordings were slightly altered by the AC-coupling of the recorder, but this had a negligible effect on the recorded waveforms. Tape-recorded EODs were subsequently digitized using the Daqbook. All digitized EODs were recorded with head-positivity upward. After recording an individual's EOD, the fish was euthanized in MS222, fixed in 10% formalin for at least 2 weeks, transferred to 70% ethanol, and deposited in the Cornell University Museum of Vertebrates. All methods conform to protocols approved by Cornell University's Center for Research Animal Resources.

Estimating EOD landmarks

Recorded EOD waveforms were analyzed using custom software written in C++. Algorithms for the detection of peaks and zero crossings in the original wave file, for the calculation of the first derivative of the

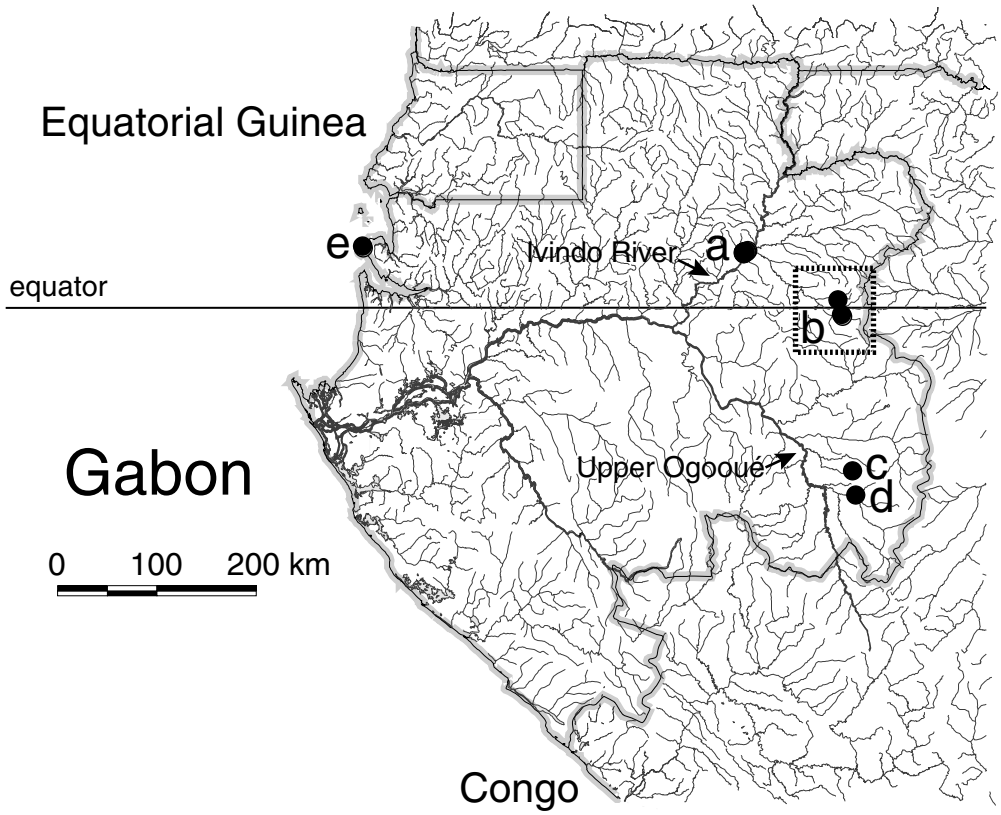

Figure 2. Drainage map of Gabon (Central Africa) showing collection localities for the seven blunt-snouted *Brienomyrus* species examined in the present study: (a) SZA, VAD, CAB, and TEN from the Makokou region of the Ivindo River; (b) SZA and CAB from streams near the Ivindo–Haut Ogooué divide; (c) PAR from Lékiye Creek in the Haut-Ogooué watershed; (d) LIS from Foumou Creek in the Haut-Ogooué watershed; and (e) LIB from coastal streams in the Estuaire province.

wave, and for the detection of peaks in the first derivative were used to estimate several EOD landmarks (Figure 3). Waves were normalized to linearly scale peak-to-peak voltages to a constant value. The time axis zero point was taken as the zero crossing (ZC2) between the maximum (P1) and minimum (P2) voltages in the wave. This landmark serves as a reference point for comparing temporal EOD parameters because it is generated, in all of these species, by inward current flow through the anterior faces of the electrocytes when they are depolarized beyond threshold by posterior face firing (Bennett 1971, Bass 1986a,c, Figure 1). The starting and ending points of the waves are ill-defined asymptotes. They were arbitrarily set at the first and last points deviating from the baseline by at least 2% of peak-to-peak voltage (Crawford & Hopkins 1989). Due to baseline noise, we only considered peaks whose absolute values were greater than 0.05% of the peak-to-peak value (for clean signals) or two times the standard deviation of the first 40 points in the waveform (for noisier signals).

For maximum (S1, S3) or minimum (S0, S2) slopes between peaks, our software returned three parameters – time of occurrence, voltage, and slope. We estimated slope as a nine-point average (with triangular weighting). Time and voltage were returned for the peak of phase 1 (P1). Time was also returned for the peak of phase 2 (P2). Voltage of P2, simply P1 voltage minus one, was omitted because it is redundant. Time and slope were returned for zero crossing 1 (ZC1). Because waves were centered on zero crossing 2 (ZC2), only slope was returned for this landmark. The times at which the wave began (T1) and ended (T2), as defined above, were also returned by the software. In addition, phase areas were calculated by numerical integration. Absolute values of all voltages between appropriate

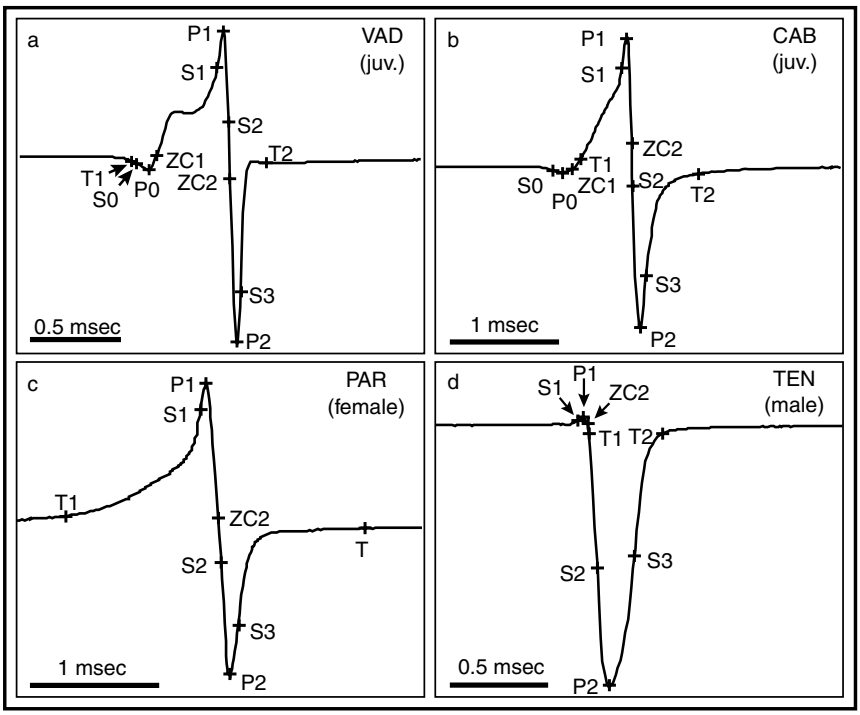

Figure 3. Examples of typical landmark data for four different kinds of EOD waveform. T1 and T2 mark the beginning and end of the wave (based on the baseline deviating by more than 2% of peak-to-peak height). S, P, and ZC refer, respectively, to maximum/minimum slope, peak, and zero-crossing for each of the different phases (indicated by 0, 1, and 2). Since all landmarks correspond to actual digitized data points, some ZC estimates deviate slightly from baseline (interpolations of landmarks were not necessary for good characterization or discrimination of waveforms). Time, voltage, and/or slope were returned for each landmark. In addition to these characters, the frequency corresponding to the maximum in the power spectrum was determined, and phase areas were estimated by numerical integration. The ordering of landmarks determined how phase areas were calculated. (a) For VAD juveniles and adult females, which emit EODs with a large initial head-negative phase, all landmarks are found, and their ordering is typical. In this case, the area of phase 0 was estimated from T1 to ZC1, and the area of phase 1 from ZC1 to ZC2. (b) When phase 0 is small, such as in the case of CAB juveniles and females, T1 may occur after S0, P0, and ZC1, in which case the area of phase 0 was calculated from S0 to ZC1. (c) PAR produces a biphasic EOD (S0, P0, and ZC1 not present; phase 0 area = 0). In this case, phase 1 area was estimated from T1 to ZC2. (d) The EOD of TEN has a very small initial head-positive phase. Whenever T1 fell after S1, phase 1 area was estimated from S1 to ZC2. Phase 2 area was calculated by numerical integration from ZC2 to T2 for all classes of EOD.

EOD landmarks (see Figure 3) were summed and divided by the sampling rate, giving phase areas in units of volt-seconds. Finally, a power spectrum of each EOD was generated by windowing the wave with a Hanning window and taking its Fast Fourier transform (Embree & Kimble 1991), from which the peak power frequency was determined.

To create a complete data set for all individuals, we dealt with missing values associated with phase 0, not being present in *Brienomyrus* sp. 'PAR' and 'TEN', in the following ways: (1) slope and voltage parameters of phase 0 landmarks were set to zero (the baseline condition); (2) times of occurrence of phase 0 landmarks were set to the means calculated for all other (triphasic) individuals included in a given analysis (the method of mean substitution), so that these landmark times would not contribute to ordination score differences; and (3) the area of phase 0 was set to zero, indicating a missing phase.

Statistical analyses

We examined relationships between characteristics of the EOD waveform and sex and/or standard length within each species. We measured standard length to the nearest mm and identified males by the presence of a notch at the base of the anal fin. This

androgen-dependent character (Iles 1960, Kirschbaum 1987, Landsman 1993a, Herfeld & Moller 1998) allows mature males, which have a notch, to be distinguished from females and immature males, which have straight anal fin bases, with little chance of false positive identification (Kramer 1997). Adult females and immature individuals were combined into a single group. Two waveform characters found in other studies to vary between sexes (Westby & Kirschbaum 1982, Landsman 1993a, Kramer 1997) or with standard length (Bass 1986c, Kramer & van der Bank 2000) were examined here: total waveform duration (= T2–T1) and peak power spectral frequency. Relationships between sex and/or standard length and these features of the EOD were explored by standard multiple regression analysis (Sokal & Rohlf 1995). A Bonferroni correction (adjusted threshold $p = 0.0018$) was applied when evaluating the significance of each standard partial regression coefficient (β).

We used principal components analysis (PCA) and discriminant function analysis (DFA) to examine variation in EOD waveform among taxa and to evaluate how well species can be classified on the basis of EOD characters alone. Thirty-two waveform variables were available for analysis. For each of the originally measured parameters, the overall sample set was first examined by constructing bar plots of all individuals, sorted by standard length and grouped by taxon and sex. This allowed us to remove parameters exhibiting little variation among species. Following Henry et al. (1999), we removed some variables that were highly correlated with others. Twenty-five variables were retained for ordination analyses.

The structure of EOD variation among individuals was examined using PCA because it does not make *a priori* assumptions about group membership (Reyment et al. 1984, Pimentel 1992). The magnitude and 'meaning' of variation in EOD waveshape captured by each principal component axis are given by its Eigenvalue (λ) and factor loadings, respectively. When EODs of different species were incompletely separated in PCA space, we used analysis of variance (Sokal & Rohlf 1995) and Scheffé's (1953) multiple comparison tests to evaluate the significance of interspecific differences in factor scores along the first two axes. The goal of linear DFA, by contrast, is to calculate a reduced number of orthogonal discriminant functions from linear combinations of the original variables, such that separation among *a priori* groups is maximized and variability within them is minimized (Reyment et al. 1984, Kleinbaum et al. 1988). We used DFA to investigate whether novel individuals can be assigned to groups (species and, in some cases, sex) on the basis of EOD characters alone. Probabilities of group membership (i.e. posterior classification probabilities) were calculated from prior probabilities of group membership and Mahalanobis generalized distances, D^2, between individual cases and group centroids, assuming standard Gaussian cumulative probability distributions (Lindeman et al. 1980).

After removing 30, randomly selected individuals from our data set, forward-stepwise DFA was performed on the remaining EODs ($n = 250$), allowing all 25 characters to enter the model. Chi-square tests were used to determine the significance of the derived canonical roots. We evaluated the power of our suite of EOD characters to discriminate *Brienomyrus* species by determining how accurately the 30 test cases, which were not used to derive the discriminant functions, were assigned to morphologically defined groups. Prior probabilities of group membership were assumed to be equal for all taxa.

We assessed the contribution of each EOD character to the discrimination of species, and in some cases sex, using partial Wilks' Λ statistics (Jennrich 1977). A lower value of partial Λ denotes a higher incremental contribution of a given variable to discrimination among groups. The relative importance (I_i) of each EOD character (i) for discriminating among *a priori* groups was also estimated as the sum, over all canonical roots, of the products of (1) the squared correlations $(r_{ij})^2$ of the individual discriminant function scores of the jth root with the measured values of the ith character and (2) the proportion of overall discrimination accounted for by each root, given by its Eigenvalue λ_j (Willig & Hollander 1995). The value of the resulting index is greatest for characters that contribute most to discrimination. We performed all statistical analyses using Statistica, release 5.1 (StatSoft, Inc., Tulsa, OK).

Results

Variation of EOD waveforms with size and sex

Electric organ discharge waveforms vary with individual size in CAB, PAR, and LIS. In addition, distinct sex differences, which have previously been described in VAD and CAB (Bass & Hopkins 1983, 1985, Bass 1986a,b), are evident in the data presented here (Figure 4). In multiple regressions of EOD duration on

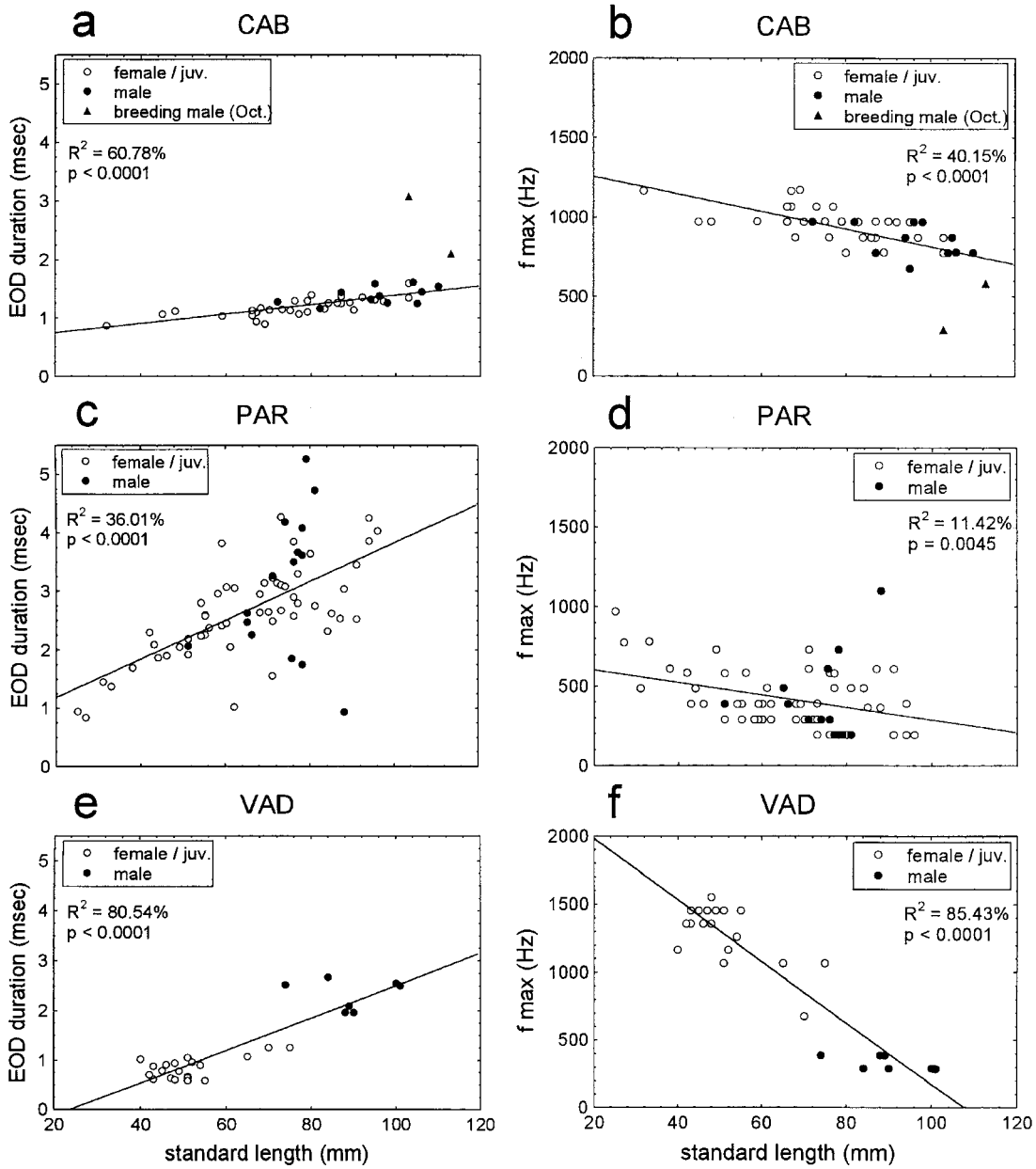

Figure 4. Variation in EOD duration (in ms) and peak power spectral frequency (f max; in Hz) with individual standard length (in mm) in three blunt-snouted *Brienomyrus* species. In all plots, open circles indicate EODs recorded from juveniles or adult females, and filled circles indicate EODs recorded from adult males. Least squares regression lines are shown for male and female data combined (R-square and p-value indicated in each plot). (a) EOD duration and (b) f max vs. standard length in CAB. In this species, filled triangles indicate two breeding males that were recorded in October and displayed seasonally-altered EOD waveforms. These two CAB males are excluded from the regression analyses shown here. (c) EOD duration and (d) f max vs. standard length for PAR. (e) EOD duration and (f) f max vs. standard length for VAD, males of which appear to undergo a permanent change in their EOD waveform when they mature sexually.

sex and standard length, we estimate significant partial regression coefficients for standard length in PAR (standardized $\beta_{SL} = 0.582, p < 0.0001$; Figure 4c) and LIS ($\beta_{SL} = 0.588, p = 0.0012$; data not shown), indicating that an increase in size accounts for an increase in EOD duration independent of the effects of sex. A marginally significant relationship between EOD duration and standard length at the Bonferroni-corrected alpha probability level is found for CAB ($\beta_{SL} = 0.463, p = 0.0026$). The significance of this association is improved when we remove two males captured in October (during Gabon's major rainy season), which displayed seasonally dimorphic EODs ($\beta_{SL} = 0.696, p < 0.0001$; Figure 4a). Similarly, an increase in standard length is associated with a decrease in the peak frequency of the EOD power spectrum of CAB ($\beta_{SL} = -0.567, p = 0.0003$; Figure 4b, two breeding males removed). A marginally significant negative association between peak power spectral frequency and standard length exists for PAR ($\beta_{SL} = -0.344, p = 0.0051$; Figure 4d). We find no evidence of a relationship between sex and either of the two-waveform characters for the above species. In the case of CAB, this likely results from the small number of breeding males with seasonally altered EODs that we recorded. By contrast, EOD duration and sex are significantly related in VAD ($\beta_{SEX} = 0.684, p = 0.0001$; $\beta_{SL} = 0.293, p = 0.0376$; Figure 4e). Both sex and standard length are independently associated with peak power spectrum frequency in this species ($\beta_{SEX} = -0.477, p = 0.0017$; $\beta_{SL} = -0.502, p = 0.0011$; Figure 4f). Unlike most other mormyrid species which change EODs seasonally, VAD males are thought to undergo a permanent EOD change at some point during their development (Bass 1986b,c).

Principal components analyses using EOD characters

The species in this study fall into two groups based on the presence or absence of P0 in their EOD waveforms (Figure 1). We have examined numerous EODs from each individual at high gain and found that PAR and TEN always produce biphasic or largely-monophasic EODs that lack P0. By contrast, individuals of the other five species always produce triphasic EODs with an initial head-negative P0. The anatomical basis for this difference is well established (Bennett 1971, Schwartz et al. 1975, Bass 1986a).

Figure 5 shows the results of a PCA of all species – both mono/biphasic (filled symbols) and triphasic (open symbols) – aimed at determining whether landmark based PCA can resolve these two classes of waveform when all species are included in the analysis. We report factor loadings and Eigenvalues in the caption of this figure, as well as those of all subsequent PCA plots. EODs recorded from TEN are distinct from those of all triphasic species in the overall analysis. However, the biphasic EODs produced by PAR overlap with the triphasic EODs of CAB, LIS, and LIB despite their diagnostic lack of P0 (Figure 5). This overlap results from: (1) the very small values for S0 voltage, P0 voltage, and phase 0 area in CAB, LIS, and LIB, which are close to the value of zero for these characters in PAR; and (2) the large EOD duration range in PAR (0.8–5.3 ms, based on 2% deviation from baseline), which encompasses those of CAB juveniles and females (0.9–1.6 ms), LIS (1.1–2.0 ms), and LIB (0.9–1.5 ms). Individuals defined as PAR do form a distinct cluster, however, in any two-species PCA performed using any one of the examined triphasic species (data not shown). Below, we present results of principal components analyses for biphasic and triphasic species separately to explore waveform variation within each of these EOD classes.

Electric organ discharges of TEN and PAR clearly differ from one another along the first principal factor axis generated from an analysis of these two biphasic species (Figure 6). This axis is most heavily loaded by variables describing the size and shape of the initial head-positive peak (P1), which clearly differs between these two species. Figure 7 shows PCA results for EODs produced by the remaining five species, all of which produce triphasic EODs. The greatly elongated male EODs of VAD and CAB are excluded from this PCA, since they form clearly distinct clusters in the overall PCA of all seven species (Figure 5). Some separation between species clusters is achieved along the first principal factor axis of Figure 7, which contrasts the time of occurrence of waveform timing landmarks that occur after the time zero reference (ZC2) with ones that occur before it. Thus, factor 1 can be thought of as an EOD duration axis. By contrast, factor 2 is most strongly loaded by several landmarks associated with the shape and relative size of the initial head-negative phase. Owing to their large P0s, VAD juveniles and adult females form a cluster which is significantly different along this dimension from those of the other four taxa ($p < 0.0001$ in all pairwise comparisons). The EODs of the only three sympatric species (SZA, VAD, and CAB) form discrete clusters in this comparison.

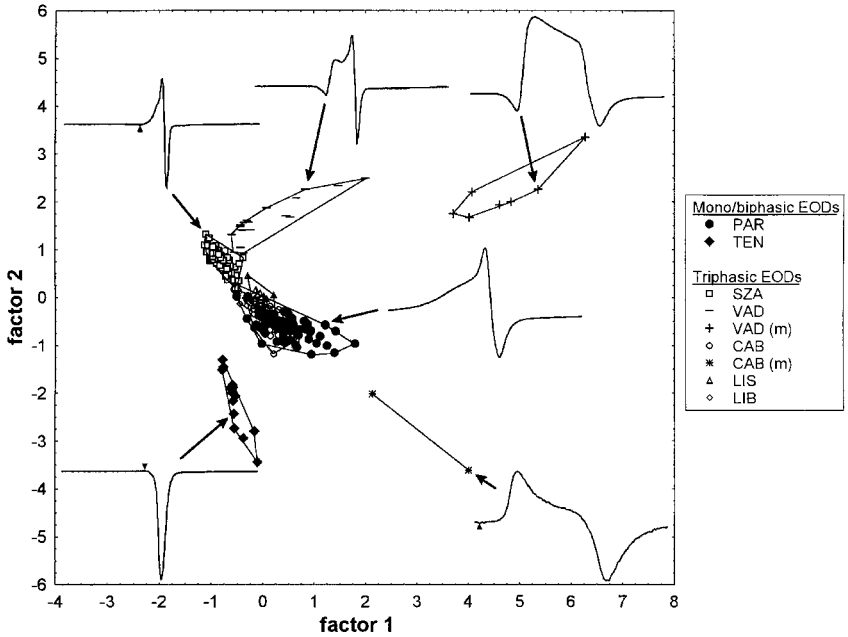

Figure 5. Plot of the first and second factor axis scores from a PCA of all seven blunt-snouted *Brienomyrus* species. The first factor axis ($\lambda_1 = 9.241$) explains 36.96% of the variance in the original data. The EOD variables that load most heavily onto this axis are complex, including phase 1 area (loading = +0.914), time of S1 (−0.877), time of P1 (−0.868), slope of S3 (−0.739), and phase 0 area (+0.714). The second principal factor axis ($\lambda_2 = 7.061$) explains an additional 28.24% of the total variance in EOD waveshape. Phase 2 area (−0.790), slope at S1 (+0.790), and voltage of S3 (+0.778) load most heavily on the second axis. Each data point represents an EOD recorded from a single individual, coded by taxon (and in some cases, sex). There are two codes for VAD ('−'= juveniles and adult females; '+'= adult males) and for CAB ('◯'= juveniles, adult females, and non-breeding males; '∗'= breeding males). All EODs (shown for specified individuals) have been scaled to a constant peak-to-peak amplitude (head-positivity up) and the same trace duration (= 3 ms). Small triangles on the traces indicate minute initial peaks that are too small to see.

Removal of VAD (females and juveniles) provides further separation among operational taxonomic units (Figure 8). Here, variables with the strongest loadings on the first and second axes are generally the same as those in the previous analysis. The principal factor axes can thereby be interpreted, again, as mostly reflecting variation in EOD duration (first factor) and the size and shape of the initial head-negative EOD phase (second factor). *Brienomyrus* sp. 'LIS' forms a distinct cluster largely on the basis of the second principal factor axis alone ($p < 0.0001$ in all pairwise comparisons). Although we observe significant differences among the remaining taxa along the first factor axis ($p < 0.005$ in all pairwise comparisons), resolution is further improved when we remove individuals morphologically defined as LIS. Figure 9 shows the results of a final PCA that only included SZA, CAB (two breeding males excluded), and LIB. These taxa produce very similar EODs (Figure 9). Based on landmark characters largely relating to EOD duration and P0 and S0, SZA, CAB, and LIB form distinct clusters in PCA space.

DFA and classification by signal waveform

Forward-stepwise DFA performed on 250 individuals, allowing all 25 EOD characters to enter the model, produces seven significant canonical roots that explain 99.87% of the total variance and provides a high degree of discrimination among the seven blunt-snouted taxa (overall Wilks' $\Lambda < 0.0001$). Using the derived classification functions, we correctly assign all 30 test cases to species. Furthermore, we are able to assign test cases of VAD adult males to species and sex. Table 1 reports the mean *a posteriori* probabilities with which we make these classifications. With two exceptions, all individuals are assigned to their correct groups with near unity probability. Although CAB (juveniles, females, and non-breeding males) and LIB (all age/sex classes) are correctly classified, low probabilities of incorrect

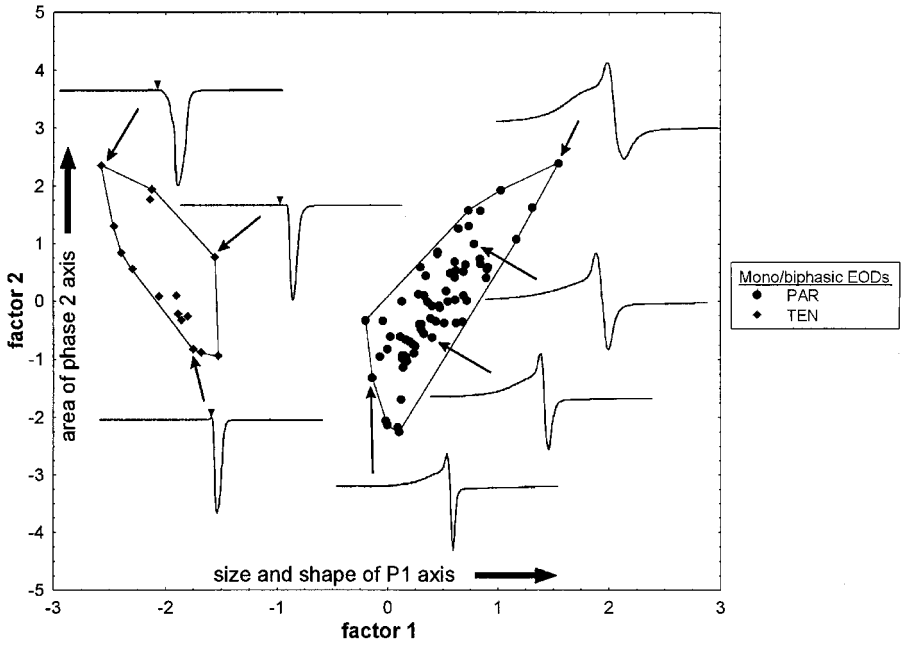

Figure 6. Plot of the first and second factor axis scores from a PCA of the two biphasic species: PAR and TEN. The first factor axis ($\lambda_1 = 9.282$) explains 54.60% of total EOD variation and is heavily loaded by variables describing the size and shape of the initial head-positive phase {P1 voltage (loading = +0.977), S1 voltage (+0.968), phase 1 area (+0.886), and slope at S1 (+0.816)}. The second factor axis ($\lambda_2 = 4.382$) explains 25.78% of the total variance and largely reflects variation in the area of phase 2 (loading = +0.838). Each data point represents an EOD recorded from a single individual, coded by taxon. EODs (scaled to a constant peak-to-peak amplitude and a trace duration of 4 ms) are shown for specified individuals (head-positivity up). The position of P1 is indicated by small triangles in the case of TEN.

reciprocal assignment are estimated for these allopatric species due to the similarity of their EODs. Values of partial Wilks' Λ and I_i (the index of importance for discrimination) indicate that most of the 25 EOD characters contribute relatively evenly to among-group discrimination (Table 2).

Discussion

Intraspecific EOD variation

A positive association between EOD duration and standard length, regardless of sex, exists for three blunt-snouted species (CAB, PAR, and LIS). Previous studies of electrocyte ultrastructure suggest that the degree of surface area proliferation of the electrocyte faces, especially the anterior face, accounts for much of the variation in EOD duration noted among mormyrid species (Bennett 1971, Bass et al. 1986). Gonadal steroid-dependent sex differences in this feature of electrocyte anatomy have also been described (Bass et al. 1986). The mechanism of size-dependent variation in EOD duration observed for CAB, PAR, and LIS remains unknown, but it may be associated with this kind of difference in electrocyte ultrastructure. It is also possible that the active electrical properties of the adult electric organ (see Zakon et al. 1999) may change during growth and contribute to waveform variation by individual standard length, but this remains to be investigated.

In contrast to size-related changes, androgen-dependent EOD sex differences are well known in many mormyrid species (Bass 1986b,c). In previous field experiments, testosterone treatments induced a lengthening of the EOD and accompanying waveform changes in VAD and CAB, but not in SZA (Bass & Hopkins 1983, 1985). Our analyses of intraspecific EOD variation in wild caught fishes are consistent with results of hormone treatment experiments in these three species. We cannot rule out the possibility of seasonal sex differences for the four other blunt-snouted

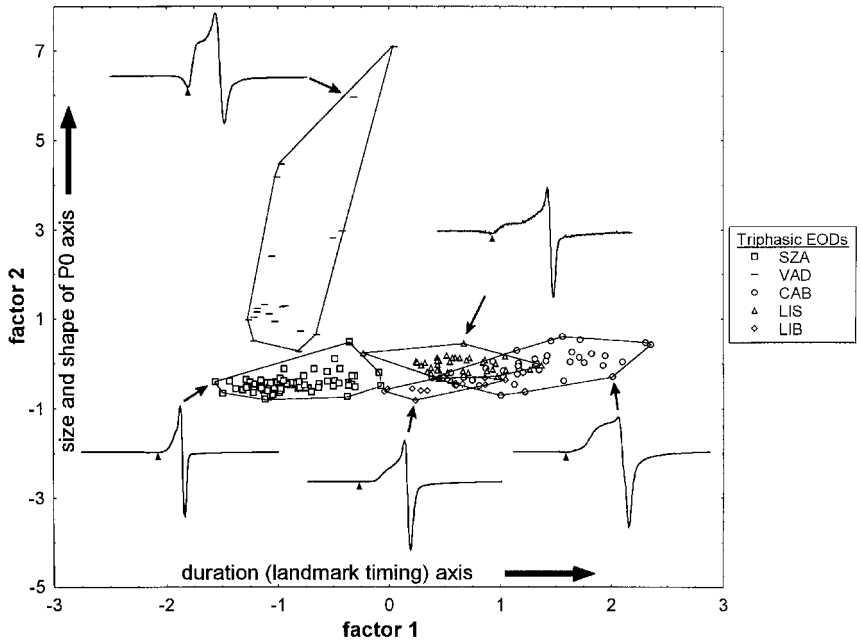

Figure 7. Plot of the scores along the first two factor axes from a PCA of five triphasic species. The first factor axis ($\lambda_1 = 11.040$) and second factor axis ($\lambda_2 = 6.471$) explain 44.16% and 25.88%, respectively, of the total variation measured in the EOD waveforms. The first axis is negatively loaded by time landmarks that occur before the time zero reference {T1 (loading= -0.762), time of P0 (-0.927), and time of ZC1 (-0.925)} and positively loaded by time landmarks that occur after the time zero reference {T2 ($+0.883$), time of P2 ($+0.849$), and time of S3 ($+0.841$)}. The peak frequency of the power spectrum (-0.850) also loads heavily onto this axis. This axis largely reflects EOD duration among the sampled waveforms. The second factor axis is strongly loaded by the area of phase 0 ($+0.942$), slope at ZC1 ($+0.941$), P0 voltage (-0.930), and S0 voltage (-0.925), all of which are associated with the size and shape of phase 0. VAD ($-$) refers only to juveniles and adult females, and CAB ($\bigcirc$) excludes two male EODs recorded during the breeding season. Otherwise, taxonomic codes include all individuals of both sexes. EOD traces (scaled to a constant peak-to-peak amplitude and a trace duration of 3 ms) are shown for some individuals (head-positivity up). In these traces, small triangles point to the position of P0.

Brienomyrus species, however, due to a lack of knowledge of their reproductive biology, and inadequate sampling during the onset of the breeding season (September–November).

Primary among environmental influences on the EOD waveform is temperature. While the effects of temperature on the EOD frequency of wave-type gymnotiforms have been relatively well characterized (Enger & Szabo 1968, Boudinot 1970, Feng 1976), few data concerning temperature effects on mormyrid EOD waveforms have been systematically collected. Harder et al. (1964) described several non-linear temperature-dependent changes in the EOD waveform of the mormyrid *Gnathonemus petersii*, including a decrease in EOD duration with increasing temperature, and Kramer & Westby (1985) applied a Q_{10} of 1.5 to temperature-correct the EODs of this species. Application of an appropriate Q_{10} factor to our EOD data would likely have reduced residual variation in the relationships between EOD duration and standard length and, perhaps, some of the scatter in our ordination plots. Unfortunately, temperature data were not consistently collected for all field recordings over the past 20 years. Temperature-dependent variation probably had a minimal effect on our results, however, due to the narrow temperature range encountered (available recording temperatures = 22–26°C) and the relatively large numbers of individuals sampled during numerous, independent collections made at different times of year (see Appendix 1). Lastly, conductivity (Harder et al. 1964, Bell et al. 1976), stress associated with captivity (Landsman 1993b), and changes in social ranking (Carlson et al. 2000) can alter the EOD waveform. These effects were avoided by recording EODs in the field with little delay, using low conductivity stream water (12–30 μS/cm) taken from the site of capture.

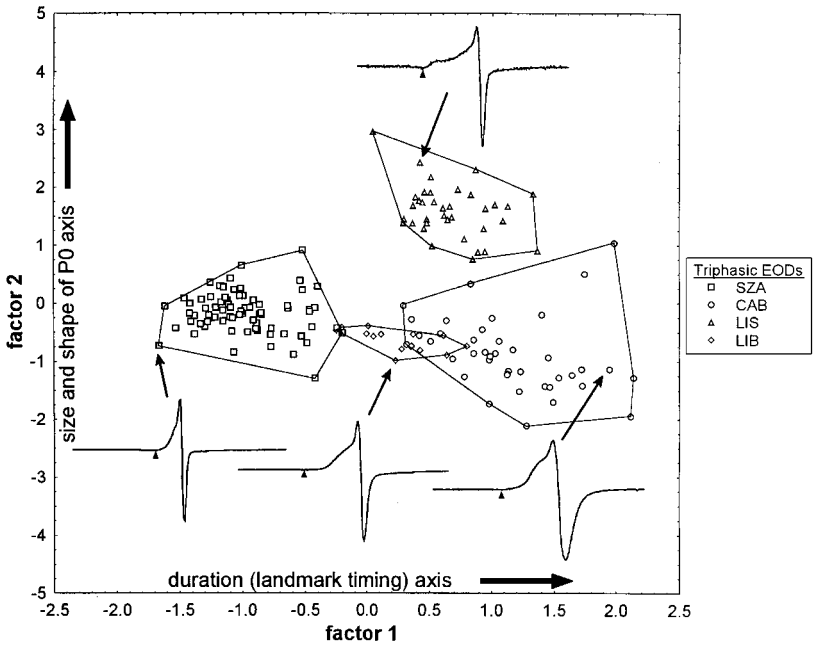

Figure 8. Plot of the first and second factor axis scores from a PCA of EODs produced by four triphasic species. The first and second axes explain 47.87% ($\lambda_1 = 11.969$) and 22.62% ($\lambda_2 = 5.656$) of the total variance in EOD waveshape, respectively. The first factor axis contrasts the timing of landmarks that occur before ZC2, the time-zero reference point {T1 (loading = −0.858), time of S0 (−0.902), time of P0 (−0.929), time of ZC1 (−0.926), and time of P1 (−0.775)} with those that occur after ZC2 {time of P2 (+0.818), time of S3 (+0.800), and T2 (+0.900)}. This axis is also heavily loaded by peak frequency of the power spectrum (−0.919). The second factor axis relates mostly to the size and shape of the initial head-negative waveform phase. The variables that load most heavily on the second axis are P0 voltage (−0.874), slope at ZC1 (+0.833), S0 voltage (−0.801), area of phase 0 (+0.770), and slope at S0 (−0.744). Each data point represents an EOD recorded from a single individual, coded by taxon. The data for CAB (◯) exclude two male EODs recorded during the breeding season. EODs (scaled to a constant peak-to-peak amplitude and a trace duration of 3 ms) are shown for specified individuals (head-positivity up). The position of P0 is indicated by a small triangle in each of the EOD traces.

EOD variation among taxa

Electric organ discharge waveforms have been considered in relatively few taxonomic studies of mormyrids. One of the characters that initially indicated *Mormyrus subundulatus* to be a new species was its EOD, which differed from that of its only sympatric congener, *Mormyrus rume* (Crawford & Hopkins 1989). Species status for *M. subundulatus* was confirmed by morphological analysis (Roberts 1989). Moller & Brown (1990) recorded two EOD types within *Mormyrops curviceps* collected from the Moa River (Sierra Leone). They reported no morphological differences between EOD forms and were unable to relate EOD differences to developmental stage or sex. More recently, Kramer & van der Bank (2000) considered EOD measurements in their description of *Petrocephalus wesselsi*.

According to Moller and Brown (1990), before EOD waveforms can be used for taxonomic discriminations among mormyrids, it must be demonstrated that the EOD is as 'rigid and invariable' as traditionally applied morphological characters and that EODs are critical to mate recognition. The EODs we recorded for this study vary intraspecifically (e.g. size-related changes in EOD duration). Nevertheless, we have demonstrated using PCA that seven blunt-snouted *Brienomyrus* species produce distinct EODs. They are sufficiently stereotyped and species-typical, in fact, that individuals can be assigned to taxa using multivariate classification functions based on EOD measurements alone.

Electric signals and species recognition

The result that blunt-snouted *Brienomyrus* species produce distinct EODs is consistent with the hypothesis that EOD waveforms serve as signals advertising species identity in this group of mormyrid fishes.

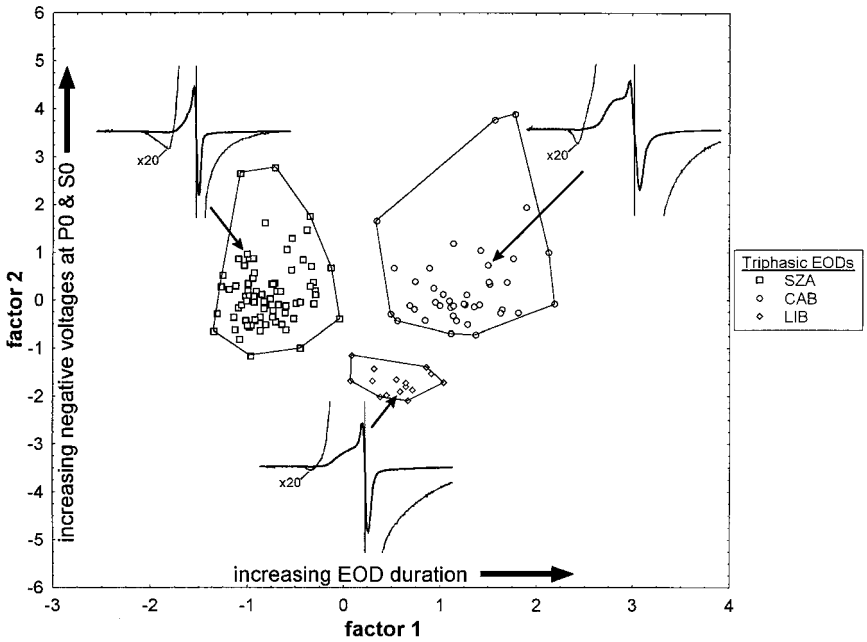

Figure 9. Plot of the scores along the first two factor axes from a PCA of blunt-snouted *Brienomyrus* species SZA, CAB, and LIB. The first and second principal factor axes account, respectively, for 55.86% ($\lambda_1 = 13.964$) and 13.41% ($\lambda_2 = 3.354$) of the variation in measured waveform characters among these species. The first axis is heavily loaded by T1 (−0.969), time of S0 (−0.912), time of P0 (−0.949), time of ZC1 (−0.947), time of P1 (−0.863), time of P2 (+0.927), time of S3 (+0.935), T2 (+0.937), and peak frequency of the power spectrum (−0.938). As in the previous analyses, this axis may be interpreted as largely reflecting EOD duration. The second factor axis is strongly loaded by only two variables reflecting the amplitude of the initial head negative phase: P0 voltage (−0.900) and S0 voltage (−0.766). Each data point represents an EOD recorded from a single individual, coded by taxon. The data for CAB (◯) exclude two male EODs recorded during the breeding season. A representative EOD (scaled to a constant peak-to-peak amplitude and a trace duration of 3 ms) is shown for each taxon (head-positivity up), along with an amplified (×20) trace for better visualization of the initial head-negative phase.

Based on behavioral studies, many species of weakly electric fish appear to be able to discriminate species, sex, and even individual differences in EOD waveforms (Hopkins & Bass 1981, Graff & Kramer 1992, McGregor & Westby 1992). Moller & Serrier (1986) demonstrated spatial orientation of mormyrid species by EOD waveform but could not eliminate other cues of potential importance. In *Pollimyrus adspersus*, on the other hand, sonic males recognize conspecific females by their highly regularized sequence of pulse intervals (SPI) rather than the waveform of their EODs (Crawford 1991). Pulse rhythm also appears to play a role in conspecific recognition for *Campylomormyrus rhynchophorus* (Kramer & Kuhn 1994).

The neural processing involved in discriminating EOD waveforms during social communication has been relatively well studied in mormyrids. Among the classes of mormyrid electroreceptors, knollenorgans function in social communication, firing spikes that are phase-locked to rapid outside negative-to-positive voltage transients (Szabo 1962, Bennett 1965, Hopkins & Bass 1981, Hopkins 1986). An EOD that causes knollenorgans to respond on one side of the body is instantaneously received by knollenorgans on the other side as a reversed-polarity EOD owing to the reversed direction of current flow (Bennett 1965, Hopkins & Bass 1981). Considering responses only to the largest voltage transients, the latency between knollenorgan firing on either side of the body in response to blunt-snouted *Brienomyrus* EODs would correspond roughly to the time difference measured between S1 and S2 (or perhaps ZC1 and ZC2) in six of the species, or between S2 and S3 in TEN. This two-spike code is conveyed from the receptors to the midbrain nucleus exterolateralis pars anterior (ELa) via the knollenorgan pathway, which is characterized by a number of anatomical and physiological adaptations for the accurate preservation of time domain information (Enger et al. 1976,

Table 1. Matrix of probabilities with which 30 novel test cases are accurately classified to species, and in some cases sex, using classification functions derived from DFA (based on 250 different individuals).

Actual taxon (sex)	# Test cases	Means (Std Dev) of Calculated Probabilities of Classification to the Indicated TAXON (sex) Based on EOD Measurements								
		SZA	VAD (juv/f)	VAD (m)	CAB	PAR	LIS	TEN	LIB	CAB (m)
SZA	10	1.000 (0.000)	0 (0.000)	0 (0.000)	0 (0.000)	0 (0.000)	0 (0.000)	0 (0.000)	0 (0.000)	0 (0.000)
VAD (juv/f)	3	0 (0.000)	1.000 (0.000)	0 (0.000)	0 (0.000)	0 (0.000)	0 (0.000)	0 (0.000)	0 (0.000)	0 (0.000)
VAD (m)	2	0 (0.000)	0 (0.000)	1.000 (0.000)	0 (0.000)	0 (0.000)	0 (0.000)	0 (0.000)	0 (0.000)	0 (0.000)
CAB	5	0 (0.000)	0 (0.000)	0 (0.000)	0.997 (0.005)	0 (0.000)	0 (0.000)	0 (0.000)	0.003 (0.005)	0 (0.000)
PAR	4	0 (0.000)	0 (0.000)	0 (0.000)	0 (0.000)	1.000 (0.000)	0 (0.000)	0 (0.000)	0 (0.000)	0 (0.000)
LIS	2	0 (0.000)	0 (0.000)	0 (0.000)	0 (0.000)	0 (0.000)	1.000 (0.000)	0 (0.000)	0 (0.000)	0 (0.000)
TEN	2	0 (0.000)	0 (0.000)	0 (0.000)	0 (0.000)	0 (0.000)	0 (0.000)	1.000 (0.000)	0 (0.000)	0 (0.000)
LIB	2	0 (0.000)	0 (0.000)	0 (0.000)	0.126 (0.173)	0 (0.000)	0 (0.000)	0 (0.000)	0.874 (0.173)	0 (0.000)
CAB (m)	0	—	—	—	—	—	—	—	—	—

Three letter abbreviations (left column), also used by Sullivan et al. (2002), correspond to working manuscript names proposed for these taxa (Teugels & Hopkins unpublished). Shown for each group of test cases (left column) are the mean (and standard deviation) of the posterior classification probabilities calculated from the prior probabilities of group membership (assumed equal for all groups) and the Mahalanobis generalized distances between individual cases and group centroids. All 30 test cases are correctly classified, but the probability of correct group assignment is less than unity for only two allopatric taxa: CAB (juveniles and adult females) and LIB (all sampled individuals).

Table 2. Indicators of the relative importance of each EOD character for discriminating among blunt-snouted *Brienomyrus* species.

EOD character, i	Partial Wilks' Λ	p-value (partial Λ)	I_i
Time of P1	0.3243	†	0.5445
Time of P0	0.9516	0.2071	0.1455
f max power	0.4700	†	0.1126
T1 (start time)	0.3169	†	0.2119
Slope at ZC1	0.6024	†	0.4672
Phase 2 area	0.5547	†	0.1711
Phase 1 area	0.4124	†	0.4835
Voltage at P1	0.6769	†	0.4105
Voltage at S1	0.7758	†	0.0533
Time of S1	0.8029	†	0.4914
Time of P2	0.6740	†	0.2752
Voltage at P0	0.5652	†	0.4344
Phase 0 area	0.5158	†	0.4591
Slope at S0	0.6001	†	0.3832
Time of S0	0.7638	†	0.1407
Time of S3	0.7746	†	0.2894
Voltage at S3	0.8056	†	0.2099
Slope at S1	0.6954	†	0.4250
Slope at ZC2	0.6615	†	0.2090
Slope at S3	0.7427	†	0.1474
T2 (end time)	0.8814	0.0005	0.1999
Voltage at S0	0.9092	0.0073	0.4445
Time of ZC1	0.9449	0.1317	0.1477
Time of S2	0.8791	0.0004	0.0796
Voltage at S2	0.9008	0.0034	0.1882

EOD characters are listed in the order in which they were added during a forward-stepwise DFA of 250 randomly chosen individuals. Partial Wilks' Λ is the multiplicative increment to Wilks' Λ (the ratio of within-groups generalized dispersion to overall generalized dispersion) resulting from stepwise variable addition during DFA. The lower this value, the greater the contribution of a character to group discrimination. P-values for the statistical significance of partial Λ's are also given († indicates $p < 0.0001$). The index of the ith character's importance for among-group discrimination, I_i, follows Willig & Hollander (1995). Higher values of I_i are associated with variables of higher discriminatory power.

Szabo et al. 1979, Bell & Grant 1989, Amagai et al. 1998). Xu-Friedman & Hopkins (1999) have proposed that cells of ELa participate in a delay-line blanking mechanism to analyze time difference in the two-spike code for the purpose of species recognition.

The only field experiment to address species recognition in mormyrids demonstrated that breeding VAD males can distinguish conspecific female EODs using a two-spike code (Hopkins & Bass 1981). Jitter at the level of ELa, which is relatively high at threshold stimulus intensities, drops to about 100 μs as stimulus intensity increases (Amagai et al. 1998). The EODs of some sympatric blunt-snouted species differ enough from one another (e.g. in waveform duration) for species recognition to be mediated by a two-spike code alone. It is unclear, however, whether a two-spike code would suffice in other cases given the measured level of jitter in ELa. If EOD field intensities generated by a conspecific at close proximity were high enough, the initial head-negative phase of some waveforms might allow for finer-scale temporal discrimination of EODs based on a three, or four, spike code. This possibility remains unexplored for the knollenorgan pathway. Other signals, such as the SPIs, may contribute importantly to the mormyrid mate recognition system when sympatric species share similar EOD waveforms.

Results of our multivariate analyses of EOD variation provide an initial indication that signal dispersion may be enhanced among sympatric species, relative to those with allopatric distributions (see Otte 1989). Among the seven blunt-snouted *Brienomyrus* species studied, allopatric taxa tend to show more overlap of their EOD waveforms in PCA space than do sympatric taxa (Figures 7 and 8). In addition, CAB and LIB have allopatric distributions, and they are the only two species for which we estimated small probabilities of incorrect reciprocal classification. Excluding the two cases of greatly elongated male EODs, the species with the most extreme variation in EOD duration noted among the taxa studied (PAR) is the sole *Brienomyrus* species that occurs where it was collected. If species recognition relies critically on the EOD waveform in the *Brienomyrus* species flock from Gabon, reproductive character displacement may be expected in zones of overlap between species sharing similar EOD waveforms. Testing this hypothesis will rely on wider geographic sampling and improved phylogenetic resolution (e.g. Sullivan et al. 2002). As these goals are achieved, multivariate analysis of EOD waveforms will contribute to the taxonomic description of newly discovered species and to a better understanding of the evolutionary mechanisms underlying signal variation in this group of mormyrids.

Acknowledgements

Permission to work at the field station in Makokou and to collect fish specimens in Gabon was granted, respectively, by P. Posso (I.R.E.T.) and J.-D. Mbega (I.R.A.F.), to whom we owe gratitude for logistical

support in Gabon. A. Georges graciously extended an invitation to C.D.H. and M. Friedman to work at C.I.R.M.F. (Franceville). Collections and EOD recordings were made over several years. For this we thank: K. Askins, R. Askins, A. Bass, C. Bell, M. Bilamba, F. Boubomba, J. Crawford, M. Friedman, G. Harned, K. Hopkins, S. Lavoué, R. Lewis, M. Marcheterre, J.-H. Mve, J. Ndong, M. Stiassny, and J. Sullivan. We are especially indebted to M. Friedman for initially writing the code in C++ that we subsequently modified to make the EOD measurements presented in this study. J. Friel catalogued our collections for the Cornell Museum of Vertebrates. B. Carlson provided helpful comments on an earlier version of this manuscript. This research was supported by funds from the National Geographic Society (5801-96; to C.D.H.), the N.S.F. (INT-9605176 and DEB-0108372; to C.D.H.), and the N.I.M.H. (MH37972; to C.D.H. and M.E.A.).

References

Alves-Gomes, J. & C.D. Hopkins. 1997. Molecular insights into the phylogeny of mormyriform fishes and the evolution of their electric organs. Brain Behav. Evol. 49: 324–351.

Amagai, S., M.A. Friedman & C.D. Hopkins. 1998. Time-coding in the midbrain of mormyrid electric fish. I. Physiology and anatomy of cells in the nucleus exterolateralis pars anterior. J. Comp. Physiol. A 182: 115–130.

Bass, A.H. 1986a. Species differences in electric organs of mormyrids: substrates for species-typical electric organ discharge waveforms. J. Comp. Neurol. 244: 313–330.

Bass, A.H. 1986b. A hormone-sensitive communication system in an electric fish. J. Neurobiol. 17: 131–156.

Bass, A.H. 1986c. Electric organs revisited: evolution of a vertebrate communication and orientation organ. pp. 13–70. *In*: T.H. Bullock & W. Heiligenberg (ed.) Electroreception, John Wiley & Sons, New York.

Bass, A.H., J.-P. Denizot & M.A. Marchaterre. 1986. Ultrastructural features and hormone-dependent sex differences of mormyrid electric organs. J. Comp. Neurol. 254: 511–528.

Bass, A.H. & C.D. Hopkins. 1983. Hormonal control of sexual differentiation: changes in electric organ discharge waveform. Science 220: 971–974.

Bass, A.H. & C.D. Hopkins. 1985. Hormonal control of sex differences in the electric organ discharge (EOD) of mormyrid fishes. J. Comp. Physiol. A 156: 587–604.

Bell, C.C., J. Bradbury & C.J. Russell. 1976. The electric organ of a mormyrid as a current and voltage source. J. Comp. Physiol. 110: 65–88.

Bell, C.C. & K. Grant. 1989. Corollary discharge inhibition and preservation of temporal information in a sensory nucleus of mormyrid electric fish. J. Neurosci. 9: 1029–1044.

Bennett, M.V.L. 1965. Electroreception in mormyrids. Cold Spring Harbor Symposia on Quantitative Biology 30: 245–262.

Bennett, M.V.L. 1971. Electric organs. pp. 347–491. *In*: W.S. Hoar & D.J. Randall (ed.) Fish Physiology, Volume 5, Academic Press, New York.

Bernard, G.D. & C.L. Remington. 1991. Color vision in *Lycaena* butterflies: spectral tuning of receptor arrays in relation to behavioral ecology. Proc. Natl. Acad. Sci. USA 88: 2783–2787.

Boudinot, M. 1970. The effect of decreasing and increasing temperature on the frequency of the electric organ discharge in *Eigenmannia* sp. Comp. Biochem. Physiol. 37: 601–603.

Bullock, T.H. & W. Heiligenberg. 1986. Electroreception, John Wiley & Sons, New York, 722 pp.

Carlson, B.A., C.D. Hopkins & P. Thomas. 2000. Androgen correlates of socially induced changes in the electric organ discharge waveform of a mormyrid fish. Horm. Behav. 38: 177–186.

Couldridge, V.C.K. & G.J. Alexander. 2002. Color patterns and species recognition in four closely related species of Lake Malawi cichlid. Behav. Ecol. 13: 59–64.

Crawford, J.D. 1991. Sex recognition by electric cues in a sound-producing mormyrid fish, *Pollimyrus isidori*. Brain Behav. Evol. 38: 20–38.

Crawford, J.D. & C.D. Hopkins. 1989. Detection of a previously unrecognized mormyrid fish (*Mormyrus subundulatus*) by electric discharge characters. Cybium 13: 319–326.

Den Hollander, J. 1995. Acoustic signals as specific-mate recognition signals in leafhoppers (Cicadellidae) and planthoppers (Delphacidae) (Homoptera, Auchenorrhyncha). pp. 440–463. *In*: D.M. Lambert & H.G. Spencer (ed.) Speciation and the Recognition Concept: Theory and Application, Johns Hopkins University Press, Baltimore.

Embree, P.M. & B. Kimble. 1991. C Language Algorithms for Digital Signal Processing. Prentice-Hall, Englewood Cliffs, New Jersey, 456 pp.

Enger, P.S., S. Libouban & T. Szabo. 1976. Fast conducting electrosensory pathway in the mormyrid fish, *Gnathonemus petersii*. Neurosci. Lett. 2: 133–136.

Enger, P.S. & T. Szabo. 1968. Effect of temperature on the discharge rates of the electric organ of some gymnotids. Comp. Biochem. Physiol. 27: 625–627.

Feng, A.S. 1976. The effect of temperature on a social behavior of weakly electric fish *Eigenmannia virescens*. Comp. Biochem. Physiol. A 55: 99–102.

Gosse, J.-P. & T. Szabo. 1960. Variation morphologique et fonctionnelle de l'organe électrique dans une même espèce de Mormyrides (*Mormyrops deliciosus* Leach). Comptes rendus hebdomadaires des Séances de l'Académie des Sciences, Paris 251: 2791–2793.

Graff, C. & B. Kramer. 1992. Trained weakly-electric fishes *Pollimyrus isidori* and *Gnathonemus petersii* (Mormyridae, Teleostei) discriminate between waveforms of electric pulse discharges. Ethology 90: 279–292.

Greenwood, P.H. 1974. Cichlid fishes of Lake Victoria, East Africa: the biology and evolution of a species flock. Bull. Br. Museum of Natural History (Zoology) 6 (Suppl): 1–134.

Harder, W., A. Schief & H. Uhlemann. 1964. Zur funktion des elektrischen organs von *Gnathonemus petersii* (Gthr. 1862) (Mormyriformes, Telesotei). Z. vergl. Physiol. 48: 302–331.

Henry, C.S., M.L. Martínez Wells & C.M. Simon. 1999. Convergent evolution of courtship songs among cryptic species of the *carnea* group of green lacewings (Neuroptera: Chrysopidae: Chrysoperla). Evolution 53: 1165–1179.

Henry, C.S., M.M. Wells & R.J. Pupedis. 1993. Hidden taxonomic diversity within *Chrysoperla plorabunda* (Neuroptera: Chrysopidae): two new species based on courtship songs. Ann. Entomol. Soc. Am. 86: 1–13.

Herfeld, S. & P. Moller. 1998. Effects of 17 α-methyltestosterone on sexually dimorphic characters in the weakly discharging electric fish, *Brienomyrus niger* (Günther, 1866) (Mormyridae): electric organ discharge, ventral body wall indentation, and anal-fin ray bone expansion. Horm. Behav. 34: 303–319.

Hopkins, C.D. 1980. Evolution of electric communication channels of mormyrids. Behav. Ecol. Sociobiol. 7: 1–13.

Hopkins, C.D. 1986. Behavior of Mormyridae. pp. 527–576. *In*: T.H. Bullock & W. Heiligenberg (ed.) Electroreception, John Wiley & Sons, New York.

Hopkins, C.D. 1999. Signal evolution in electric communication. pp. 461–491. *In*: M.D. Hauser & M. Konishi (ed.) The Design of Animal Communication, MIT Press, Cambridge, MA.

Hopkins, C.D. & A.H. Bass. 1981. Temporal coding of species recognition signals in an electric fish. Science 212: 85–87.

Hunsaker, D. 1962. Ethological isolating mechanisms in the *Sceloporus torquatus* group of lizards. Evolution 16: 62–74.

Iles, R.B. 1960. External sexual differences and their significance in *Mormyrus kannume* Forskal. 1775. Nature 188: 516.

Jennrich, R.I. 1977. Stepwise discriminant analysis. pp. 76–95. *In*: K. Enslein, A. Ralston & H.S. Wilf (ed.) Statistical Methods for Digital Computers (vol. III of Mathematical Methods for Digital Computers), John Wiley & Sons, New York.

Kirschbaum, F. 1987. Reproduction and development of the weakly electric fish, *Pollimyrus isidori* (Mormyridae, Teleostei) in captivity. Environ Biol. Fish. 20: 11–31.

Kleinbaum, D.G., L.L. Kupper & K.E. Muller. 1988. Applied regression analysis and other multivariable methods, 2nd edition, PWS-Kent Publishing Co, Boston, 718 pp.

Kramer, B. 1997. A field study of African elephantfish (Mormyridae, Teleostei): electric organ discharges in *Marcusenius macrolepidotus* (Peters, 1852) and *Petrocephalus catostoma* (Günther, 1866) as related to sex. J. Afr. Zool. 111: 313–341.

Kramer, B. & B. Kuhn. 1994. Species recognition by the sequence of discharge intervals in weakly electric fishes of the genus *Campylomormyrus* (Mormyridae, Teleostei). Anim. Behav. 48: 435–445.

Kramer, B. & F.H. van der Bank. 2000. The southern churchill, *Petrocephalus wesselsi*, a new species of mormyrid from South Africa defined by electric organ discharges, genetics, and morphology. Environ Biol. Fish. 59: 393–413.

Kramer, B. & G.W.M. Westby. 1985. No sex difference in the waveform of the pulse type electric fish, *Gnathonemus petersii* (Mormyridae). Experientia 41: 1530–1531.

Landsman, R.E. 1993a. Sex differences in external morphology and electric organ discharges in imported *Gnathonemus petersii* (Mormyriformes). Anim. Behav. 46: 417–429.

Landsman, R.E. 1993b. The effects of captivity on the electric organ discharge and plasma hormone levels in *Gnathonemus petersii* (Mormyriformes). J. Comp. Physiol. A 172: 619–631.

Landsman, R.E., C.F. Harding, P. Moller & P. Thomas. 1990. The effects of androgens and estrogen on the external morphology and electric organ discharge waveform of *Gnathonemus petersii* (Mormyridae, Teleostei). Horm. Behav. 24: 532–553.

Lavoué, S., R. Bigorne, G. Lecointre & J.-F. Agnèse. 2000. Phylogenetic relationships of mormyrid electric fishes (Mormyridae: Teleostei) inferred from cytochrome b sequences. Mol. Phylogenet. Evol. 14: 1–10.

Lindeman, R.H., P.F. Merenda & R.Z. Gold. 1980. Introduction to bivariate and multivariate analysis, Scott, Foresman & Co., Oakland, New Jersey, 444 pp.

Linn, C.E. Jr. & W.L. Roelofs. 1995. Pheromone communication in moths and its role in the speciation process. pp. 263–300. *In*: D.M. Lambert & H.G. Spencer (ed.) Speciation and the Recognition Concept: Theory and Application, Johns Hopkins University Press, Baltimore.

McGregor, P.K. & G.W.M. Westby. 1992. Discrimination of individually characteristic electric organ discharges by a weakly electric fish. Anim. Behav. 43: 977–986.

Moller, P. 1995. Electric fishes: history and behavior, 1st edition, Chapman & Hall, New York, 584 pp.

Moller, P. & B. Brown. 1990. Meristic characters and electric organ discharge of *Mormyrops curviceps* Roman (Teleostei: Mormyridae) from the Moa River, Sierra Leone, West Africa. Copeia 1990: 1031–1040.

Moller, P. & J. Serrier. 1986. Species recognition in mormyrid weakly electric fish. Anim. Behav. 34: 333–339.

Morse, D. & E. Meighen. 1986. Pheromone biosynthesis and role of functional groups in pheromone specificity. J. Chem. Ecol. 12: 335–351.

Otte, D. 1989. Speciation in Hawaiian crickets. pp. 482–526. *In*: D. Otte & J.A. Endler (ed.) Speciation and its Consequences, Sinauer Associates, Inc., Sunderland, MA.

Otte, D. 1994. The crickets of Hawaii: origin, systematics and evolution, The Orthopterists' Society, Academy of Natural Sciences of Philadelphia, Philadelphia, 396 pp.

Pimentel, R.A. 1992. An introduction to ordination, principal components analysis and discriminant analysis. pp. 11–28. *In*: J.T. Sorensen & R. Foottit (ed.) Ordination in the Study of Morphology, Evolution and Systematics of Insects: Applications and Quantitative Genetic Rationals, Elsevier, New York.

Reyment, R.A., R.E. Blackith & N.A. Campbell. 1984. Multivariate morphometrics, 2nd edition, Academic Press, New York, 233 pp.

Roberts, T.R. 1989. *Mormyrus subundulatus*, a new species of mormyrid fish with a tubular snout from West Africa. Cybium 13: 51–54.

Scheffé, H. 1953. A method for judging all contrasts in the analysis of variance. Biometrika 40: 87–104.

Schwartz, I.R., G. Pappas & M.V.L. Bennett. 1975. The fine structure of electrocytes in weakly electric teleosts. J. Neurocytol. 4: 87–114.

Seehausen, O. & J.J.M. van Alphen. 1998. The effect of male coloration on female choice in closely related Lake Victoria cichlids (*Haplochromis nyererei* complex). Behav. Ecol. Sociobiol. 42: 1–8.

Shaw, K.L. 2000. Further acoustic diversity in Hawaiian forests: two new species of Hawaiian cricket (Orthoptera: Gryllidae: Trigonidiinae: *Laupala*). Zool. J. Linn. Soc. 129: 73–91.

Sokal, R.R. & F.J. Rohlf. 1995. Biometry: the Principles and Practice of Statistics in Biological Research, 3rd edition, W. H. Freeman & Co., New York, 887 pp.

Sullivan, J.P., S. Lavoué & C.D. Hopkins. 2000. Molecular systematics of the African electric fishes (Mormyroidea: Teleostei) and a model for the evolution of their electric organs. J. Exp. Biol. 203: 665–683.

Sullivan, J.P., S. Lavoué & C.D. Hopkins. 2002. Discovery and phylogenetic analysis of a riverine species flock of African electric fishes (Mormyridae: Teleostei). Evolution 56: 597–616.

Szabo, T. 1962. Spontaneous electrical activity of cutaneous receptors in mormyrids. Nature 194: 600–601.

Szabo, T., P.S. Enger & S. Libouban. 1979. Electrosensory systems in the mormyrid fish, *Gnathonemus petersii*: special emphasis on the fast conducting pathway. J. Physiol. (Paris) 75: 409–420.

Westby, G.W.M. & F. Kirschbaum. 1982. Sex differences in the waveform of the pulse-type electric fish, *Pollimyrus isidori* (Mormyridae). J. Comp. Physiol. 145: 399–403.

Willig, M.R. & R.R. Hollander. 1995. Secondary sexual dimorphism and phylogenetic constraints in bats: A multivariate approach. J. Mammal. 76: 981–992.

Xu-Friedman, M.A. & C.D. Hopkins. 1999. Central mechanisms of temporal analysis in the knollenorgan pathway of mormyrid electric fish. J. Exp. Biol. 202: 1311–1318.

Zakon, H., L. McAnelly, G.T. Smith, K. Dunlap, G. Lopreato, J. Oestreich & W.P. Few. 1999. Plasticity of the electric organ discharge: implications for the regulation of ionic currents. J. Exp. Biol. 202: 1409–1416.

Appendix 1. List of specimens for which EODs were recorded and analyzed.

Species	Collection localities	Dates	CU catalog #s	#Individ.
SZA n = 75	Balé Ck. (Ogooué-Ivindo) 0°31′ 11.0″ N, 12°47′ 55.5″ E	Sep, 1994	75368, 75370, 75371, 75388, 75389, 75390, 75391, 77401, 77402, 77403	28
	Ivindo R. (Ogooué-Ivindo) 0°33′ N, 12°51′ E	Sep, 1994	75369	1
	Ivindo R. below Loa-Loa (Ogooué-Ivindo) 0°31′14.6″N, 12°49′20.3″ E	Jan, 1998	80842	8
	Balé Ck., multiple sites (Ogooué-Ivindo)	Jan, 1998	80843, 80845, 80848, 80849, 80861, 80933	28
	Ivindo R. at Loa-Loa Rapids (Ogooué-Ivindo) 0°31′16″ N, 12°49′28″ E	Jan, 1998	80844	4
	Nyame Pendé Ck. (Ogooué-Ivindo) 0°30.135′ N, 12°47.80′ E	Jan, 1998	80847, 80895, 80898	4
	Stream near Makatabongoy Village, Ivindo R. (near border between Ogooué-Ivindo & Haut-Ogooué) 0°08′9.6″S, 13°43′0.1″ E	Feb, 1998	80846	2
VAD n = 27	Upper Balé Ck. (Ogooué-Ivindo) 0°30′58″ N, 12°47′38″ E	Sep, 1994	75417, 75418, 77404, 77405, 77406	22
	Nyame Pendé Ck. (Ogooué-Ivindo) 0°30.135′ N, 12°47.80′ E	Jan, 1998	79704	1
	Upper Balé Ck. (Ogooué-Ivindo) 0°30′58″ N, 12°47′38″ E	Feb, 1998	80857	4
CAB n = 43	Balé Ck. (Ogooué-Ivindo) 0°31′11.0″ N, 12°47′55.5″ E	Oct, 1981	81009	3
	Balé Ck. (Ogooué-Ivindo) 0°31′11.0″ N, 12°47′55.5″ E	Oct, 1993	Field#1031 (93–004)	1
	Balé Ck., two sites (Ogooué-Ivindo)	Sep, 1994	75382, 75383, 75397, 77397	6
	Ivindo R. (Ogooué-Ivindo) 0°31.4595′ N, 12°48.3514′ E	Jan, 1998	80813	1
	Nyame Pendé Ck. (Ogooué-Ivindo) 0°30.135′ N, 12°47.80′ E	Jan, 1998	80853	1
	Nyame Pendé Ck. (Ogooué-Ivindo) 0°30.135′ N, 12°47.80′ E	Jan, 1998	80896, 80897	3
	Balé Ck., multiple sites (Ogooué-Ivindo)	Jan-Feb, 98	80811, 80812, 80815, 80816, 80850, 80855	13
	Stream along Makokou-Okondja highway, Ivindo R. (Ogooué-Ivindo) 0°09′54.1″ N, 13°37′56.0″ E	Feb, 1998	80856	3
	Stream along Makokou-Okondja highway, Ivindo R. (near border between Ogooué-Ivindo & Haut-Ogooué) 0°06′02.7″ S, 13°41′46.7″ E	Feb, 1998	80858, 80864	6
	Stream near Makatabongoy Village, Ivindo R. (near border between Ogooué-Ivindo & Haut-Ogooué) 0°08′9.6″ S, 13°43′0.1″ E	Feb, 1998	80860	6

Appendix 1. (Continued)

Species	Collection localities	Dates	CU catalog #s	#Individ.
PAR n = 69	Lékiye Ck. (Haut-Ogooué) 1°21′9.5″ S, 13°46′21.7″ E	Nov, 1993	75456, 75457, 75475, 77315, 77316	28
	Lékiye Ck. (Haut-Ogooué) 1°21′9.5″ S, 13°46′21.7″ E	Aug, 1999	80933	41
LIS n = 36	Foumou Ck. at Onkouafalla Vill. (Haut-Ogooué) 1°47′35.0″ S, 13°49′53.0″ E	Nov, 1993	75470, 75471	13
	Foumou Ck. at Onkouafalla Vill. (Haut-Ogooué) 1°47′35.0″ S, 13°49′53.0″ E	Aug, 1999	81090	23
TEN n = 15	Ivindo R. at IRET (Ogooué-Ivindo) 0°31.5′ N, 12°48′ E	Sep, 1994	75403, 80805	3
	Balé Ck. (Ogooué-Ivindo) 0°31′11.0″ N, 12°47′55.5″ E	Sep, 1994	75364, 77407	2
	Balé Ck., two sites (Ogooué-Ivindo)	Jan, 1998	80809, 80814	3
	Ivindo R. below Loa-Loa (Ogooué-Ivindo) 0°31′14.6″ N, 12°49′20.3″ E	Jan, 1998	80807	2
	Ivindo R. at Loa-Loa Rapids (Ogooué-Ivindo) 0°31′16″ N, 12°49′28″ E	Jan, 1998	80806, 80808	5
LIB n = 15	Stream near Cap Santa Clara (Estuaire) 0°33′4.7″ N, 9°20′48.0″ E	Feb, 1998	80867	13
	Stream near Cap Esterias (Estuaire) 0°35′5.1″ N, 9°20′5.2″ E	Aug, 1999	80804	2
Grand total				280

Shown from left to right are: taxon designations; localities and dates of collection; CU (Cornell University Museum of Vertebrates) catalog numbers; and number of specimens collected and recorded in each case.